CHEMMAT 796 Research Masters Thesis

Adsorptive removal of volatile anaesthetics from waste gas using biochar

Oliver Doube

A thesis submitted in fulfilment of the requirements of Master of Engineering (Research) in Chemical and Materials Engineering, the University of Auckland, 2022

ABSTRACT

This thesis evaluated biochar as a potential novel adsorbent for capturing the anaesthetic agent, sevoflurane, from medical waste gas. Because sevoflurane is a potent greenhouse gas, its capture is deemed vital to reducing the healthcare industry's emissions while also achieving the sustainable goal of reducing waste and making anaesthesia more efficient. Biochar was hypothesised to be a promising adsorbent of anaesthetic gases because it has abundant surface oxygen functionality. Original biochar was initially characterised and found to have an apparent specific surface area much lower than desired for an adsorbent of gases, so it was further engineered to increase these physical properties without altering the chemical surface character. Unfortunately, it was concluded that biochar is not a suitable adsorbent, with zero adsorbent capacity being measured for original biochar, heat-treated biochar or heat-treated biochar subjected to a hydrothermal treatment. A geometrical incompatibility between the target molecule and the pore size of the adsorbent could cause this poor performance, with the lack of chemical interactions between the target molecule and other substances also contributing. Therefore, activated carbon remains the best performing material, and recommendations for future research were made following these conclusions.

TABLE OF CONTENTS

LIST OF FIGURES

LIST OF TABLES

1 INTRODUCTION

When emitted into the atmosphere, fluorinated anaesthetic agents are greenhouse gases with a global warming potential more potent than CO_2. The healthcare community noted this harmful effect starting from, at the latest, 1989 [1], and discussions and conversations about this problem continue in the present [2]. Of known fluorinated anaesthetic agents, sevoflurane has the lowest global warming potential. Over 95% of the sevoflurane inhaled by a patient is not metabolised and is exhaled again, chemically unchanged [3]. Consider the discussion and recommendations in [4], which advocates individual anesthetists to avoid specific agents, choose more environmentally friendly alternatives and rethink whether it is necessary to use inhalational anaesthesia for a particular patient. These recommendations could mean that sevoflurane will become increasingly popular while other inhalational anaesthetic agents fall into disfavour. Indeed this could already be the case: as recently as 2014, sevoflurane made up the largest proportion of emissions among the modern inhalational anaesthetics [5].

In 2017, on a global scale, the World Health Organisation reportedly made capturing anaesthetic agents a strategic priority [6]. Research groups from various countries have been working towards that end. Previous work has used various materials as the adsorbent in an adsorption system, such as zeolites, metal-organic frameworks and activated carbon, with activated carbon being the most effective material of those already evaluated for this application using the unit operation of adsorption [7]. Another approach to capture is to use membrane technology, and recent work has been conducted in Australia to retain the anaesthetic agent in the anaesthetic circuit [8].

This thesis investigates the problem of capturing the anaesthetic agent, sevoflurane, using the unit operation of adsorption by evaluating the technical efficacy of a material novel for the adsorption of volatile anaesthetic agents with relations being made to the relevant material's physical and chemical properties. The material chosen was biochar, which is derived from biomass, and, being a carbonaceous material, is similar to activated carbon, differing in the degree to which it has been engineered. Biochar could be considered a precursor to activated carbon.

2 LITERATURE REVIEW

2.1 Target Molecule: Sevoflurane

The fluorinated anaesthetic agent targeted for capture is sevoflurane, whose chemical structure is illustrated in Figure 1, with a 3D structure depicted in Figure 2. As can be seen, sevoflurane is an ether compound with several carbon-fluorine bonds. Among modern inhalational anaesthetic agents in current clinical usage, sevoflurane has been said to approach an ideal anaesthetic agent because of the following clinical properties: it is safe, interfaces well with other medications, is effective as an anaesthetic agent for a wide variety of patients across their lifespan, provides minimal irritation to the body, in particular the passages of the airway, and it has good mass transfer properties, in particular, its low blood-gas solubility enables rapid onset and recovery from anaesthesia [9]. Furthermore, sevoflurane has good physical properties, with vapour pressure and boiling point being such that it is compatible with existing anaesthetic vapourisation technology. These properties contribute to the relative popularity of the agent in modern anaesthesia. However, sevoflurane lasts for 1.1 years in the atmosphere and has a Global Warming Potential of 130. These harmful properties justify the current work, particularly given the quantity (1200 tonnes) of sevoflurane estimated to be emitted into the atmosphere in 2014, a figure only set to increase as sevoflurane increasingly displaces other inhalational anaesthetics in clinical use [5]. Other relevant properties of sevoflurane include its density, 1.505 g/ml at 25°C, molecular weight, 200.05 g/mol [10] and its kinetic diameter, estimated to be 7.1 Å [8]. Table 1 tabulates the physical properties of sevoflurane reported in this paragraph.

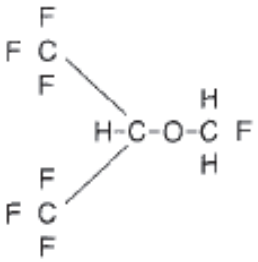

Figure 1: Chemical structure of sevoflurane, [11]

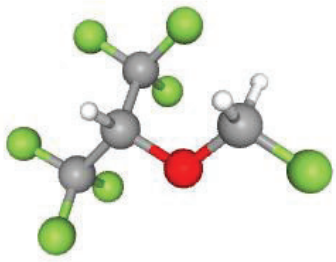

Figure 2: Sevoflurane Ball and Stick Model [10] Key: Green – fluorine, white – hydrogen, grey – carbon, red – oxygen.

Table 1: Physical Properties of Sevoflurane

Property	Value
Molecular Weight	200.05 g/mol
Boiling Point	58.5°C
Density	1.505 g/cm^3
Kinetic Diameter	7.1 Å
Vapour Pressure	25.7312 kPa at 25°C
Global Warming Potential (100 years, kg CO_2 equivalent per kg)	130
Atmospheric Lifetime	1.1 years

Sevoflurane has the lowest global warming potential of known anaesthetic agents. Additionally, because the only halogen that sevoflurane is chemically composed of is fluorine, the effect of sevoflurane on ozone depletion is minimal to zero. Other inhalational anaesthetic agents contain the other halogens, such as chlorine or bromine, which contribute to ozone depletion, as does nitrous oxide, N_2O, which is used along with oxygen as a carrier [5].

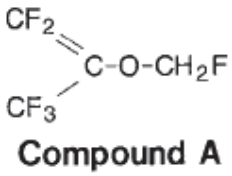

Figure 3: Chemical structure of compound A, [11]

It would be remiss to continue this discussion without mentioning the degradation product, Compound A, depicted in Figure 3. Upon encountering a strongly alkaline or basic substance, such as that used to adsorb CO_2, it has been reported that sevoflurane degrades to the so-called Compound A [11-13]. Indeed, this degradation product's formation means sevoflurane deviates from the ideal anaesthetic agent [14]. Compound A is a compound toxic to mammals, with the LC_{50} for rats reported to be 1090 ppm for a 1-hour exposure [11]. Previously, the toxicity of compound A has been reported to have caused some controversy regarding the safety of sevoflurane, although to date, "extensive clinical testing [has] failed to demonstrate any hepatic or renal dysfunction in humans" [12]. In other words, prior experience has proven sevoflurane to be a safe medication, with degradation to Compound A being so minute during historical operation of anaesthetic equipment so as not to cause adverse effects to the patient.

Nonetheless, the potential toxicity of Compound A is cause for concern. Although Compound A has previously caused no reported harm in a clinical or research setting, that does not mean that this will always be the case.

Both sevoflurane and Compound A have many carbon-fluorine bonds, and because of these bonds have chemical properties essential to understanding the underlying mechanism of interactions with other materials in processes like adsorption. No literature could be found that directly described sevoflurane's interactions with other materials; however, there is literature that makes general points about the nature of organofluorines. An excellent and short review of organofluorine chemistry makes the following point. While the carbon-fluorine bond is highly polarised, this does not result in the overall molecule having a good ability to interact with other molecules because of that fluorine [15]. In other words, interactions between organofluorine molecules and the environment are usually weaker electrostatic interactions, such as van der Waals forces, rather than hydrogen or pi-bonding interactions. One molecule famous for its non-interaction with its environment is polytetrafluoroethylene, the non-stick coating protected under the name of Teflon™.

As part of the modelling conducted within [16], in their supplementary material, the authors have published a figure that shows that the sigma profile of sevoflurane falls firmly within the non-polar region, being neither a hydrogen bond acceptor nor donor. Therefore, in keeping with the information presented in the previous paragraph, sevoflurane likely interacts with other molecules and materials solely by relatively weak electrostatic attractions.

2.2 Previous Work Capturing Sevoflurane

There is a dearth of literature related to capturing anaesthetic agents like sevoflurane. Since the papers [7, 16-21] commenced with the comprehensive review [7], another approach has been introduced to the literature. In this approach, membrane separation is used rather than adsorptive separation. The only commercial presence of anaesthetic gas capture was introduced in Canada [7], which uses adsorption.

2.2.1 Membrane Retention Approach

The membrane retention group takes a different approach to prior work. Rather than seeking to capture the volatile anaesthetic agent before it is emitted to the atmosphere, the team instead proposes a method of retaining the unmetabolised anaesthetic agent in the breathing circuit, thereby reducing the amount of anaesthetic agent wasted by reducing the amount of anaesthetic agent used, and demonstrates its efficacy in a proof of concept [8]. Their conceptual solution is compared to an existing anaesthetic circuit in Figure 4. The authors note that this system has the advantage over the adsorbent system in that it does not consume adsorbent, saving costs incurred. One disadvantage this paper has is that they do not demonstrate their proposed solution with it being integrated with an anaesthetic machine.

Another disadvantage in their paper is the relationship between the membrane and Compound A, the toxic degradation product previously mentioned in 2.1. The authors demonstrate a clear relationship between the permeance of gas molecules across the membrane and the kinetic diameter of the gas species permeating [8].

Therefore, it stands to reason that Compound A would also be retained within the anaesthetic circuit and increase over time to a concentration potentially toxic to the human patient. This safety concern is a considerable drawback of their system and goes unmentioned in their paper. However, membrane separation could be comparably effective to adsorptive separation.

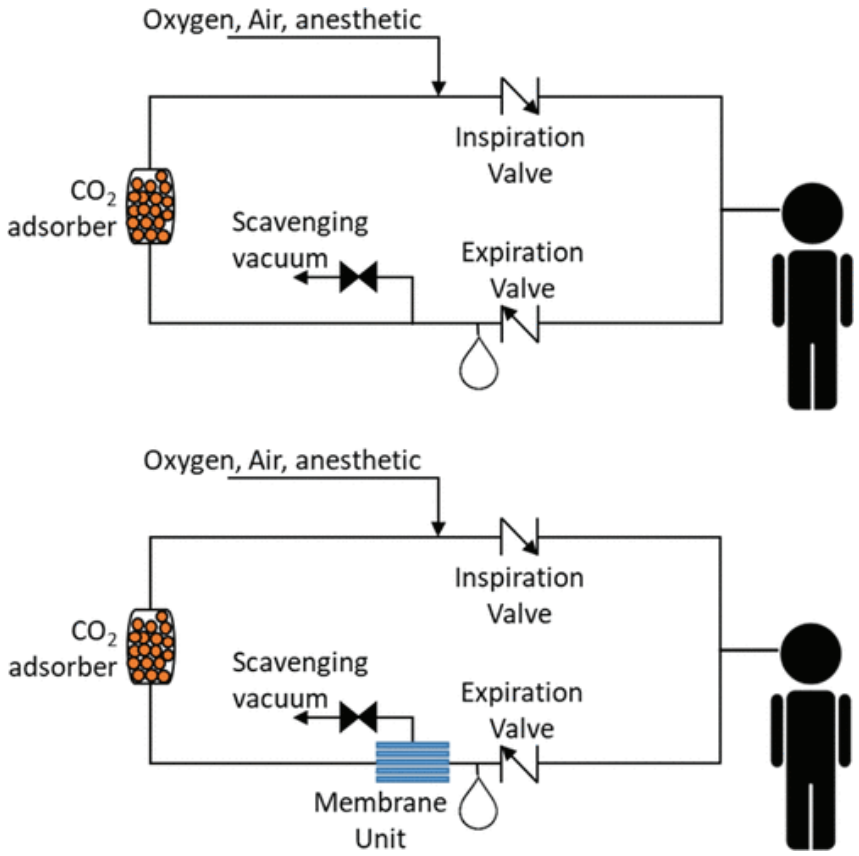

Figure 4: Schematic of the anaesthetic circuit (top) and the membrane-retention anaesthetic circuit (below), [8]

2.2.2 Adsorptive Separation Approach

The other approach to the problem of capturing anaesthetic agent emissions, more popular in the literature, is to use an adsorption system. Various adsorbent systems for numerous adsorbents have been evaluated over recent decades, including activated carbons [19, 20, 22], zeolites [22-26], metal-organic frameworks [27], aerogels [28] and porous molecular crystals [29]. The most effective material reported thus far is activated carbon, be it unmodified, as in [20] or modified with oxygenated groups, as in [16] and [19]. While Deltasorb®, the Canadian zeolite, has a reported adsorption capacity of ~400mg/g [27], the adsorption capacity of unmodified and hydrothermally modified activated carbons was ~600mg/g and 672mg/g, respectively [19]. As reported in the literature, the adsorption system types, adsorbent concentrations, adsorption system conditions, and adsorption capacities for sevoflurane are summarised in Table 2. The adsorption capacities have been standardised to be in the units of milligrams of adsorbate per gram of adsorbent. The adsorption systems are

either static systems, where adsorbent and adsorbate are mixed and allowed to reach equilibrium, or dynamic, where the adsorbate is entrained by a gas that flows through the adsorbent.

Table 2: Adsorption System Capacities from various sources in the literature.

Adsorbent Material	Type of Adsorption System	Concentration of Adsorbate	Adsorption System Conditions	Adsorption Capacity (mg/g)	Reference
		Activated Carbons			
GCA-48	Isothermal Static	~5%v/v	295 K 23.1% RH	530	[22]
RB40M	Isothermal Static	~5%v/v	295 K 23.1% RH	430	[22]
Vapour 410	Isothermal Static	~5%v/v	295 K 23.1% RH	530	[22]
H-GAC	Dynamic	3.5%v/v	Bed height = 5cm Flow Rate = 3L/min	350	[20]
E-GAC	Dynamic	3.5%v/v	Bed height = 5cm Flow Rate = 3L/min	575	[20]
Hydrothermal E-GAC	Dynamic	3.5%v/v	Bed height = 10cm Flow Rate = 3L/min	672	[19]
		Zeolites			
13x	Isothermal Static	~5%v/v	295 K 23.1% RH	330	[22]
4x	Isothermal Static	~5%v/v	295 K 23.1% RH	27	[22]
96096	Isothermal Static	~5%v/v	295 K 23.1% RH	23	[22]
Deltazite®	Isothermal Dynamic	1% v/v	298K 50% RH	320	[30]
Deltazite®	Isothermal Static	1% v/v	298K	400	[27]
13x-APG	Isothermal Static	0.95%v/v	298 K	472	[26]

Adsorbent Material	Type of Adsorption System	Concentration of Adsorbate	Adsorption System Conditions	Adsorption Capacity (mg/g)	Reference
HCZP200E	Isothermal Static	0.99%v/v	298 K	88	[26]
HCZP900E	Isothermal Static	0.99%v/v	298 K	32	[26]
		Metal-Organic Frameworks			
Cr-based MOF (MIL-101 Pellet)	Isothermal Dynamic	1% v/v	298K 50% RH	900	[30]
Cr-based MOF (MIL-101 Powder)	Isothermal Static	1% v/v	298K	>1500	[27]
Fluorinated trispyrazole-based MOF	Isothermal Static	Saturated in Nitrogen gas flow	298 K, N_2 flow	595	[29]
		Silica Gels			
Type A	Static	~5%v/v	295 K 23.1% RH	430	[22]

Although previous work [16, 17, 19] has demonstrated that surface modification of activated carbon was possible, it remains unclear to what extent surface modification affects the adsorptive properties of activated carbon. Within [19], which used the software COSMO-RS, the simulation indicates that there should be a large difference in the adsorption ability of an unmodified, activated carbon material when compared to an oxygenated activated carbon. However, experimentally, the unmodified activated carbon material had an adsorption capacity of 612 mg/g, while the best oxygenated activated carbon had an adsorption capacity of 672 mg/g. The similarity of these values is made more apparent by comparing the adsorption capacity on a surface area basis, with values for unmodified activated carbon and oxygenated activated carbon being 0.517 mg/m^2 and 0.523 mg/m^2, respectively. The success of the modification was verified using the technique of X-Ray Photoelectron Spectroscopy (XPS).

Most appropriate breakthrough model

The three breakthrough models of the Bohart-Adams, Thomas and Yoon-Nelson defined and used in [20] are mathematically analogous to one general logistic equation, equation [2.1], whose two parameters, p and q, can be used to obtain particular physical variables of the system [31]. Therefore, the usage of this general logistic model is planned to predict breakthrough characteristics of the adsorption material within this work.

$$\frac{C_t}{C_0} = \frac{1}{1 + \exp(p - qt)} \quad [2.1]$$

Where:

t is the time the fluid has been flowing through the bed, measured in seconds.

C_t is the adsorbent concentration, measured in %volume/volume, at the time, t,

C_0 is the adsorbent concentration of influent, measured in %volume/volume.

p and q are fitting parameters.

2.3 Unit Operation: Adsorption

Adsorption is the unit operation where a substance becomes distributed between a fluid and another material, known as the sorbent. Generally, sorption occurs when a molecule, known as the adsorbate or solute, accumulates or depletes in concentration at an interface, with adsorption being an accumulation of material and desorption being depletion. The interface might be gas-liquid, liquid-liquid, gas-solid and liquid-solid [32]. In the application examined in this thesis, the interface is gas-solid.

Typically, the incidence of adsorption is restricted to the interfacial surface between the sorbent and the adsorbate. Thus, the materials preferred for adsorption are highly porous, with pores that present a large surface area where the adsorbate can adsorb [32]. The surface upon which the adsorption occurs is frequently not uniform but instead suffers from heterogeneity: the physical differences, chemical differences or a combination of physical and chemical differences between areas of the material influence this heterogeneity [32]. Therefore chemical bonding energies between sorbent and adsorbate may vary widely from one location to another, even on the same material [32].

Adsorption can be classified as either physical adsorption, *physisorption,* or chemical adsorption, *chemisorption*. These two mechanisms differ by the type of physiochemical surface interaction. In physisorption, only van der Waals' interactions form between adsorbate and adsorbent, while in chemisorption, there is a formation of ionic, covalent or coordinate bonds and a corresponding change in chemical identities [32]. The difference between the two mechanisms means that they differ in a couple of critical properties. In general, physisorption is reversible, rapid and does not require activation energy, whereas chemisorption is irreversible, slow and requires an activation energy barrier to be overcome.

The performance of an adsorbent bed can be evaluated by considering the concept of the breakthrough curve, which is the concentration of adsorbate in the effluent normalised by its concentration in the feed plotted against time [33]. An exemplar of a breakthrough curve is given in Figure 5. To summarise, the fluid feed begins entering the bed at the time t_0, and at this time, a measure of the concentration of the effluent's adsorbed species reveals that the feed's adsorbed component is zero because the adsorbent bed is fully adsorbing that component. As time progresses, adsorbate concentration will increase in a characteristic logistical curve shape. The breakthrough time, t_b, is often taken to be at a time when the normalised concentration is equal to 0.05. At that time, the adsorbate has broken through the adsorbent bed, and the normalised concentration of adsorbate in the effluent will rapidly increase its saturation value to 1.0.

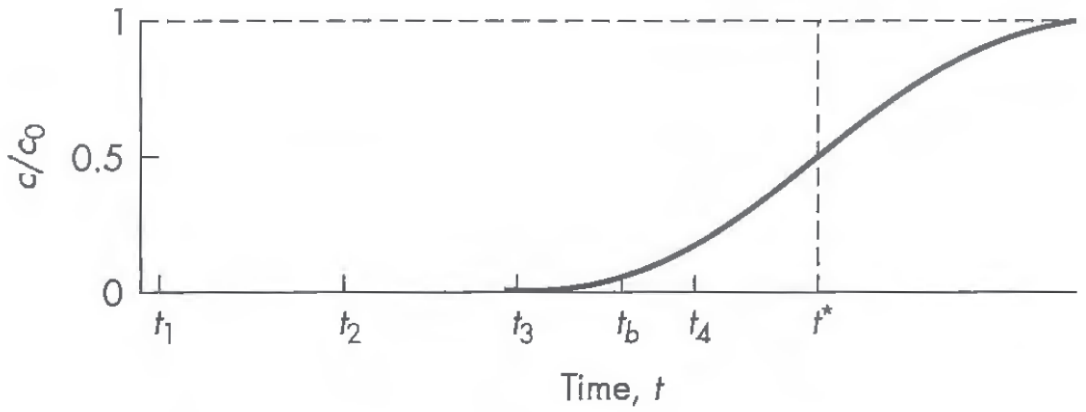

Figure 5: Breakthrough curve for adsorbent in a fixed-bed system, [33]

2.4 Proposed Material: Biochar

Biochar is a carbon-rich material with a high aromatic composition produced by biomass pyrolysis in an inert or anoxic atmosphere [34]. Biochar is an ancient material that humans have used for thousands of years. When produced from woody biomass, it is better known as 'charcoal' [35].

Figure 6: The biomass-biochar-activated carbon spectrum.

Both biochar and activated carbon are materials derived from biomass due to a degradation of the organic qualities of the source material. As biomass is engineered towards activated carbon, it could be said to pass through phases of pristine biochar and then engineered biochar. This concept is illustrated in Figure 6. Therefore,

there is a question about differentiating biochar from activated carbon. In other words, what distinguishes biochar from activated carbon; where does the dividing line get drawn on this continuum to be able to call each of these a different material?

Activated carbon is produced in a two-step process: firstly, it is carbonised, being heated to temperatures below 800°C in an inert atmosphere then; secondly, it is activated, be that physical activation, with an oxidising agent of oxygen, CO_2 or steam at higher temperatures [7], or chemical activation, with numerous chemical agents being available [36]. Therefore activated carbon is a derivative of engineered biochar [37]. This thesis defines activated carbon as engineered biochar physically activated at temperatures above 800°C or the chemically activated equivalent. Thus biochar is a material that has not been subjected to those treatments.

As it is a material that has been less processed than activated carbon, biochar has been lifecycle assessed to have a lesser environmental impact than activated carbon [38]. Economically, biochar has been reported to have a slightly lower production cost per tonne than activated carbon [39]. Both of these are desirable elements. Biochar could be a viable material in anaesthetic agent capture, granted that it has adequate adsorption performance in this application.

Regarding the physical structure of biochar, there is an illustrative diagram published in [40], reproduced herein as Figure 7, which relates the molecular structure of biochar to an increase in the charring temperature. To summarise that diagram, the biomass is initially composed of amorphous lignin, crystalline cellulose and amorphous hemicellulose, which converts into a transition char during the first charring process, with pyrogenic amorphous carbon increasing in phase fraction as it forms from the components mentioned earlier. Then, as temperature increases, the char enters a distinct amorphous char stage, composed only of pyrogenic amorphous carbon with pore space increasing with temperature. The final stage is composite char, with an increasing turbostratic crystallite phase, increasing pore space and decreasing pyrogenic amorphous carbon.

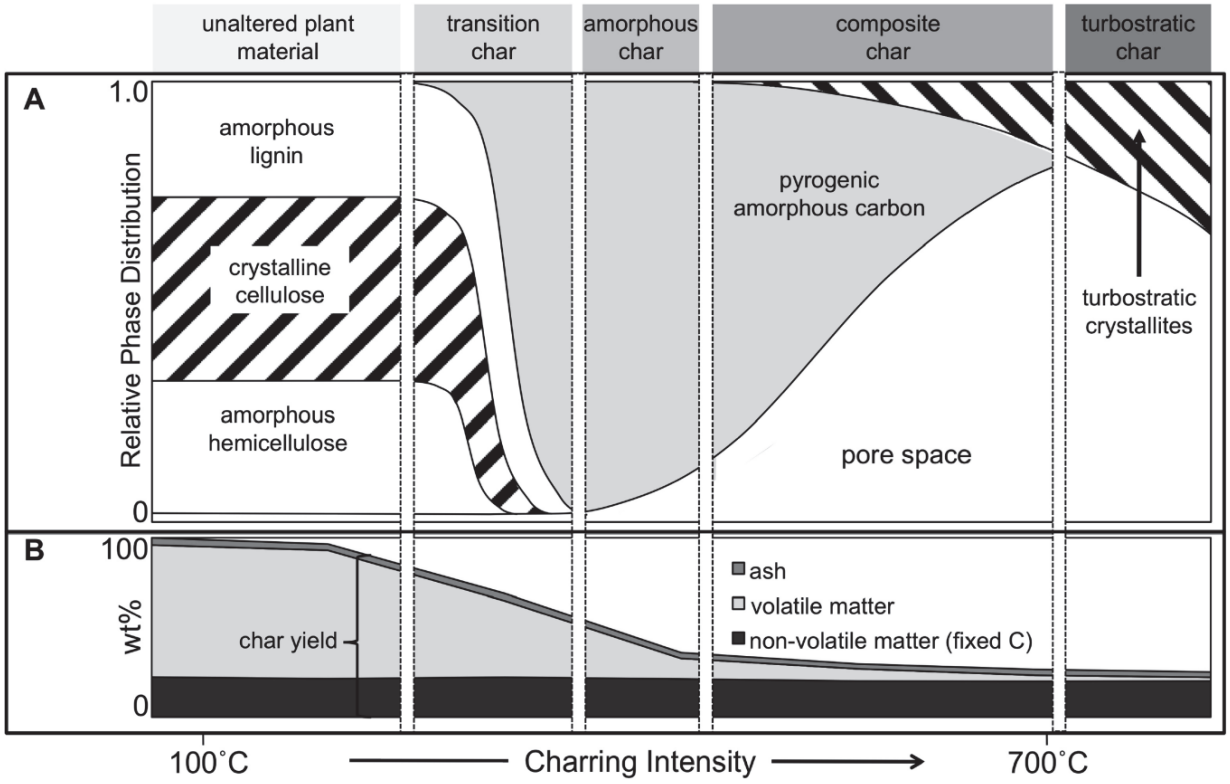

Figure 7: Dynamic molecular structure of plant-biomass derived Biochar, [40]

3 EXPERIMENTAL

The following steps were performed to obtain biochar from biomass and evaluate its adsorption performance in the anaesthetic gas adsorption system: Firstly, the biochar was produced and prepared via pyrolysis of biomass and sieving. This biochar was initially physically characterised for surface area via isothermal nitrogen adsorption and also characterised for chemical functional groups via FTIR-ATR. Thirdly, the surface area was improved via the physical activation of biochar via inert gas heat treatment. This step involved finding the best condition for heat treatment using small samples. Fourthly, sufficient material for the adsorption trials was produced using the best condition identified from the results obtained during the third step. Fifthly, the heat-treated biochar with the improved surface area was hydrothermally modified to alter its surface functional groups to be more conducive to anaesthetic gas adsorption. Three biochar materials were obtained from these five steps: 1) original biochar, 2) heat-treated biochar, and 3) hydrothermally treated biochar.

Finally, the adsorption performance of the biochar was evaluated using the anaesthetic gas adsorption system. In the top of Figure 8, Kanuka woodchip biomass can be seen, with their biochar product in the bottom part of the image.

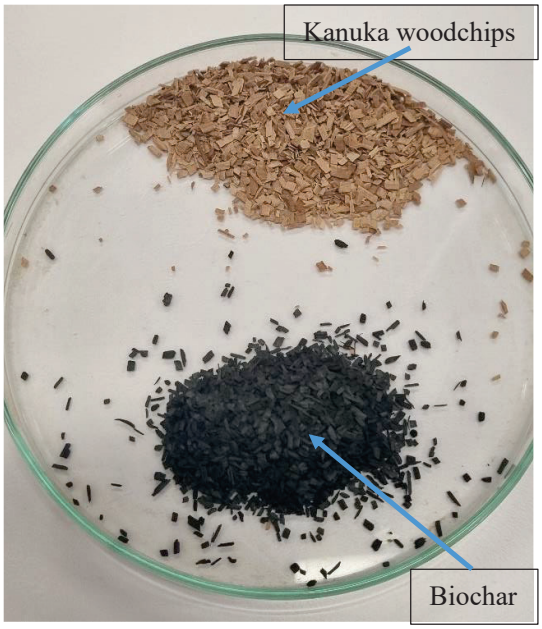

Figure 8: Kanuka woodchips and Kanuka biochar in a petri-dish

3.1 Biochar Production and Preparation

3.1.1 Methodology

The biochar material was obtained as the waste product when Kanuka (*Kuzea ericoides*) wood chips were converted into liquid smoke, as described in [41], and a recount of that method follows:

The provider harvested the Kanuka wood from New Zealand's East Cape and then converted it into wood chips of particle size 0.5 – 3.0 mm using a wood chipper. The woodchips were then commercially packaged in bags. In order to pyrolyse the woodchips, a laboratory-scale continuous pyrolyser was used. A flow diagram describing the flow of material through the pyrolyser is depicted in Figure 9, with a photograph in Figure 10.

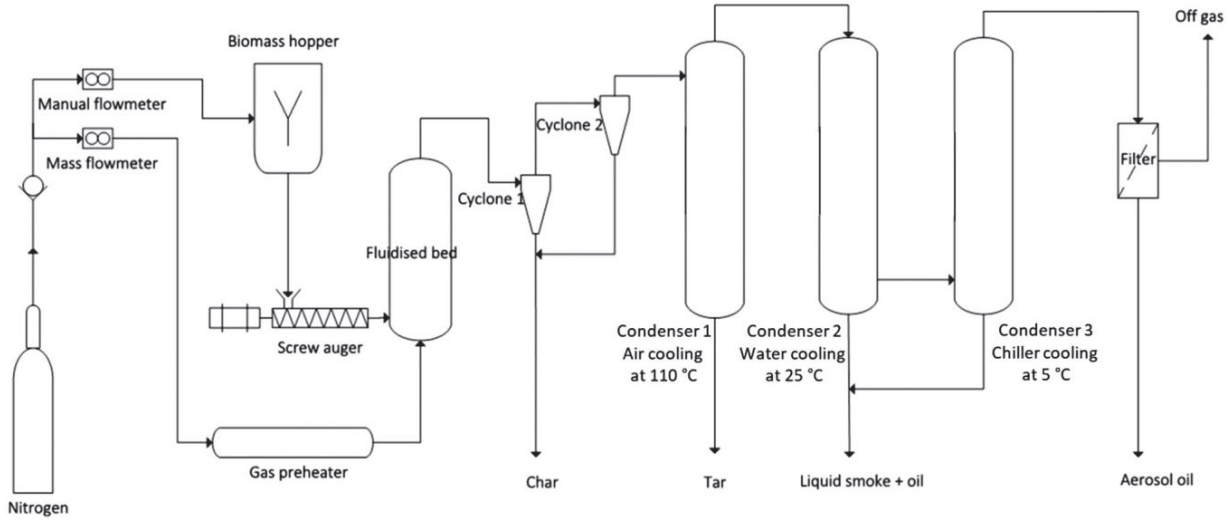

Figure 9: Flow diagram of the fluidised bed reactor used to pyrolyse the biomass, [41]

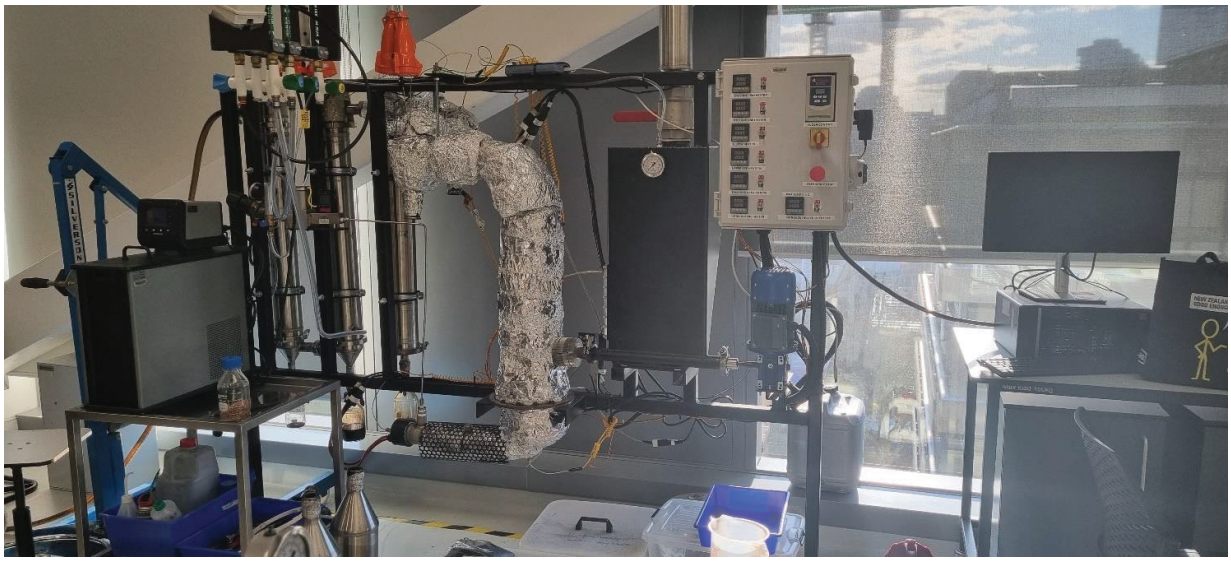

Figure 10: The fluidised bed reactor in the lab with cyclones detached

The biomass conversion into biochar occurred through three main stages – loading, pyrolysis and collection. Approximately 4 kg of kanuka woodchips were preloaded into the biomass hopper, and the fluidised bed was preheated to the target temperature of 450°C. Nitrogen gas flowed through the gas preheater, set to 420°C at a flow rate of 60 L/min, and then into the reactor bed to fluidise the silica sand. Wood chips were fed into the fluidised bed via a screw auger at 1 kg/h, and fast pyrolysis converted the wood chips to hot vapour and solid biochar in the bed. The flow of heated nitrogen entrained the vapour and particles and carried them through two

successive cyclones, which separated the solid biochar from the vapour. These cyclones were maintained at 350 – 400°C to ensure the separation occurred. The biochar was retrieved from the cyclones, allowed to cool, and sealed in a zip-lock plastic bag.

The biochar was sorted into appropriate particle sizes using four sieves and a receiver in preparation for subsequent experiments. The four sieves were arranged one above the other in order of increasing aperture, as depicted in Figure 11. Biochar was used to fill the top sieve pan to a height of approximately 1/3rd. The biochar was then sieved at an amplitude of 2 mm, 5 seconds on, 5 seconds off, for 10 minutes. The fractions were then sorted. The fraction which passed through the 1.68 mm gauge mesh but was retained by the 1.0 mm gauge mesh was stored in a sealed zip-lock plastic bag for further experimentation.

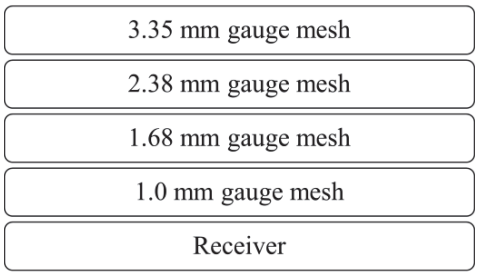

Figure 11: Sieve aperture order and sizes

3.1.2 Results

The distribution by weight percentage of the materials from the pyrolyser was 19.2% biochar, 33.2% pyrolytic liquid, 6.2% tar, 18.3% aerosol oil, and 23.1% pyrolytic gas. The size distribution of the particles retained by each sieve was not recorded. However, the fraction saved was chosen because it was the largest and, therefore, the most practical choice to continue with further experiments. 450g of biochar was obtained in the size range mentioned earlier after sieving.

3.2 Biochar Characterisation

For ease of reading, the methods of biochar characterisation will be described in this section, and the specific results of each characterisation method will be presented in this document as those results are compared in their relevant sections.

3.2.1 Method of Physical Characterisation

Apparent Surface Area and Pore Size

The following method was sourced from [4] to obtain results comparable comparison with prior work. In order to obtain a measurement of apparent surface area, the BET surface area method was followed. A 3Flex Surface Characterisation Analyser (Micromeritics Instrument Corporation, Norcross, USA) used an N_2 adsorption-desorption cycle at 77 Kelvin. Before analysis, each sample was degassed at 300°C under a vacuum for at least 6 hours using a VacPrep 061 Degasser (Micromeritics Instrument Corporation, Norcross, Georgia, USA). Then, the BET equation [3.1] was applied to the data collected at relative pressures between 0.01 and 1.0 to obtain the apparent specific surface area (SA_{BET}) according to the theory first presented in [42].

$$\text{Non-Linear Form: } q_{\text{eq}} = \frac{q_s C_{BET} C_{eq}}{(C_s - C_{eq})\left[1+(C_{BET}-1)\left(\frac{C_{eq}}{C_s}\right)\right]} \qquad [3.1]$$

$$\text{Linear Form: } \frac{C_{eq}}{q_{eq(C_s-C_{eq})}} = \frac{1}{q_s C_{BET}} + \frac{(C_{BET}-1)}{q_s C_{BET}} . \frac{C_{eq}}{C_s}$$

$$\text{Plot: } \frac{C_{eq}}{q_{eq(C_s-C_{eq})}} = \text{m}\frac{C_{eq}}{C_s} + \text{c, where m} = \frac{(C_{BET}-1)}{q_s C_{BET}}; \text{c} = \frac{1}{q_s C_{BET}}$$

Where:

q_{eq}= amount of adsorbate in the adsorbent at equilibrium

q_s = theoretical isotherm saturation capacity

C_{eq} = Adsorbate concentration at equilibrium

C_{BET}: BET adsorption isotherm relating to energy of surface interaction

C_s= Adsorbate monolayer saturation concentration

The adsorption average pore diameter was then estimated by applying the equation [3.2].

$$\sigma = \frac{4\,V_T}{\text{SA}_{\text{BET}}} \qquad [3.2]$$

Where:

σ = pore size diameter, metres. Reported in Å.

V_T= Total Pore Volume, measured in m^3/g.

SA_{BET} = Specific Surface Area by BET, measured in m^2/g.

Porosity Estimation

In order to estimate the porosity by the apparent micropore volume (V_{micro}), t-plot analysis was applied to the data obtained by the 3Flex Surface Characterisation Analyser [43].

3.3 Heat Treatment of Biochar – Optimisation of Conditions

3.3.1 Methodology

A tubular furnace was used for heat treatment of biochar under an inert atmosphere. The objective was to increase the surface area of the biochar by removing residual moisture and other volatile material.
Approximately 3 g of biochar was loaded into a crucible with a maximum volume of 42.3 cm^3 (dimensions L = 9.4 cm, H = 1.5 cm, W = 3 cm) and carefully placed at the centre of the tubular furnace, with blocks of porous ceramic on each side. The tube was then sealed, and a vacuum pump and argon gas cylinder with flow controls were used to replace the ambient environmental atmosphere with one of argon.

The heating routine was programmed on the furnace's controller the according to the same general scheme, described as follows: the tube and its contents were heated up to the target temperature at a constant heating rate, maintained at that temperature for a set amount of time, and then cooled back down to allow for the sample to be safely removed.

Effect of Time on Surface Area at Constant Temperature

An initial experiment was conducted to ascertain the time required for heat treatment. In this experiment, one temperature and two times were considered. The temperature chosen was 600°C, and the two times chosen for heat treatment were 1 hour and 2 hours. The surface area of the heat-treated biochar was then compared to the surface area of the original biochar.

Effect of Temperature on Surface Area at Constant Time

The effect of temperature was examined after deciding on an appropriate heat treatment time. For the optimisation process, three temperatures were selected: 550°C, 650°C and 750°C. The labels, experimental conditions and temperature programs for each run are presented in Table 3.

Table 3: Labels, Experimental Conditions and Temperature Programs

Label	Temperature (°C)	Atmosphere	Time (min)	Temperature Program
R1	550	Inert (Ar)	60	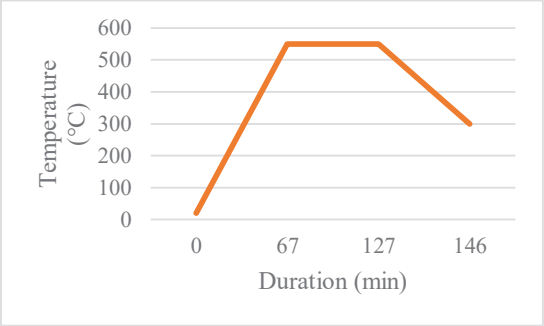
R2	550	Inert (Ar)	60	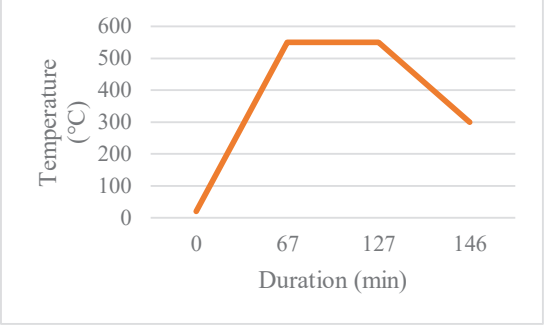
R3	650	Inert (Ar)	60	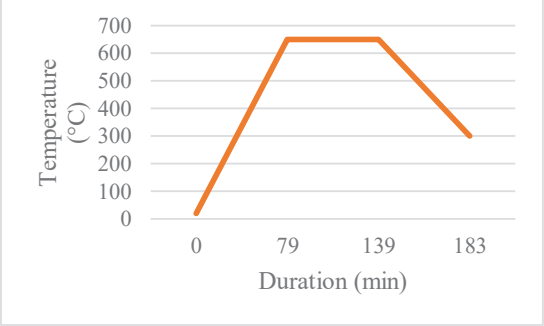
R4	650	Inert (Ar)	60	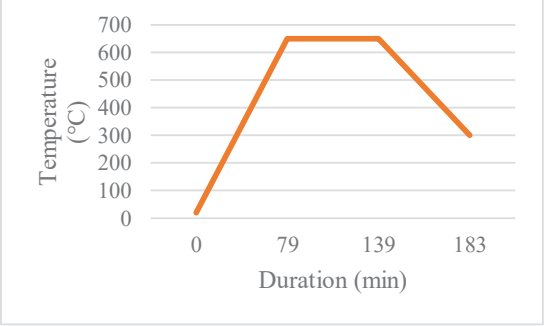

R5	750	Inert (Ar)	60	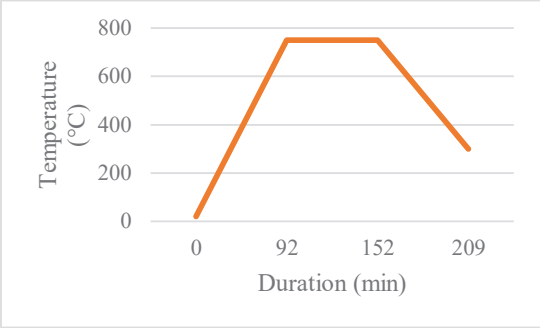
R6	750	Inert (Ar)	60	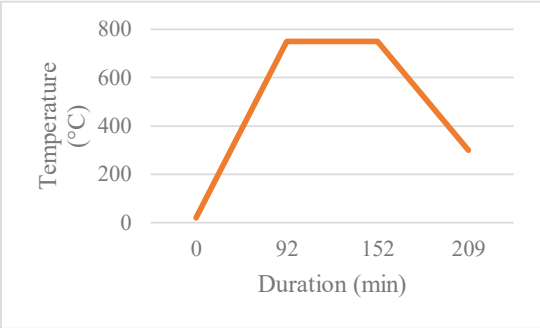

Effect of Temperature on Chemical Functionality at Constant Time

An FTIR spectrometer with universal ATR attachment was used to obtain spectrums to evaluate functional groups present on the biochar material. The instrument used was a Perkin-Elmer (Perkin-Elmer, Waltham, Massachusetts, USA), and the software used to interpret the results was PerkinElmer Spectrum-IR.

A background sample was obtained, and then each sample was placed in the centre of the top plate such that it covered the crystal. The pressure arm with a shoe attached was used to apply appropriate force to each sample to obtain an adequate spectrum.

Heat Treatment of Biochar using the best conditions

After choosing the best heat treatment temperature and time, sufficient biochar for adsorption trials was produced by repeating the heat treatment process with crucibles full of biochar. The crucible had a capacity of 8.3g. In total, 38.9g of biochar was obtained after heat treatment, and that biochar was stored in a ziplock plastic bag and mixed well before characterisation or adsorption measurement.

3.3.2 Results

Effect of Time on Surface Area at Constant Temperature

Table 4 indicates the initial and final amounts of material for each treatment time, mass loss, and yield.

Table 4: Mass Yield for each Heat Treatment Condition

Heat Treatment Condition	Initial mass (g)	Final mass (g)	Mass Loss (g)	Mass yield (%)
600°C, 1 hour	3.1225	2.5982	0.5243	83.2
600°C, 2 hours	3.1639	2.6379	0.5260	83.4

Table 5 reports the specific surface area, SA_{BET}, the micropore volume, V_{micro}, and the pore size diameter in Å of the three biochars compared at this methodology stage. This table reports that original biochar has a lower specific surface area and micropore volume than the two heat-treated samples and a larger pore size diameter than the two heat-treated samples. The heat-treated samples are broadly comparable in terms of these physical properties.

Table 5: Physical Characteristics of Biochar from heat treatment: variable time, constant temperature

Heat Treatment Condition	SA_{BET} (m^2/g)	V_{micro} (cm^3/g)	Pore Size Diameter (Å)
Original Biochar (450°C)	1.4388	0.000962	52.4793
600°C, 1 hour	376.9966	0.118485	Not Available
600°C, 2 hours	380.0259	0.138039	17.1690

Effect of Temperature on Surface Area at Constant Time

Table 6: Physical Characteristics of Biochar post-heat treatment: constant time, variable temperature

Heat Treatment Condition	SA_{BET} (m^2/g)	V_{micro} (cm^3/g)	Pore Size Diameter (Å)
Original Biochar (450°C)	1.4388	0.000962	52.4793
R1 – 550°C, 1 hour	286.0741	0.076311	18.5285
R2 – 550°C, 1 hour	268.0972	0.077622	17.4832
R3 – 650°C, 1 hour	582.3741	0.179797	16.4927
R4 – 650°C, 1 hour	435.3592	0.156171	16.4282
R5 – 750°C, 1 hour	441.2307	0.159807	16.4722
R6 – 750°C, 1 hour	466.7891	0.166013	16.4735

Table 6 reports the biochar materials' specific surface area, micropore volume, and pore size diameter. Figure 12, Figure 13 and Figure 14 depict the relationships between the average values of these properties with temperature.

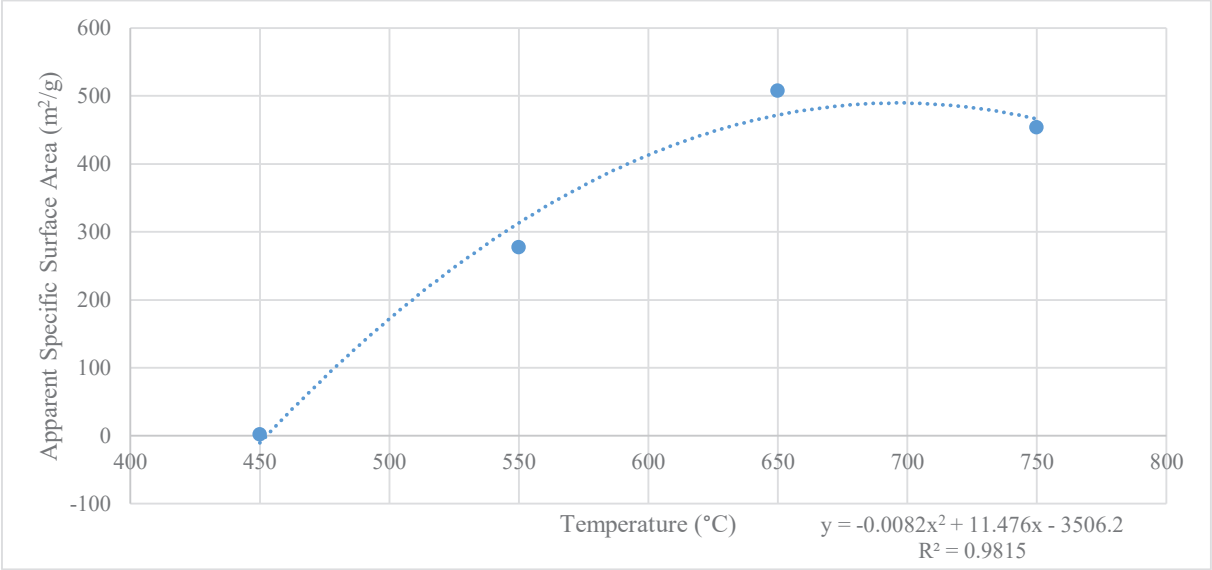

Figure 12: Biochar apparent specific surface area graphed as a function of temperature

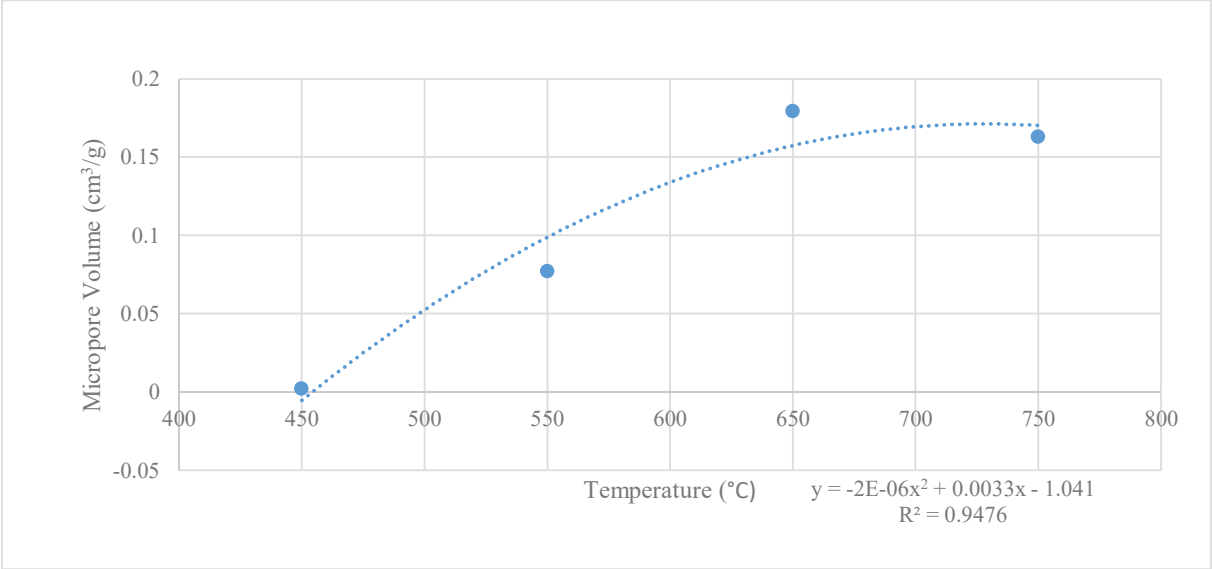

Figure 13: Biochar micropore volume graphed as a function of temperature

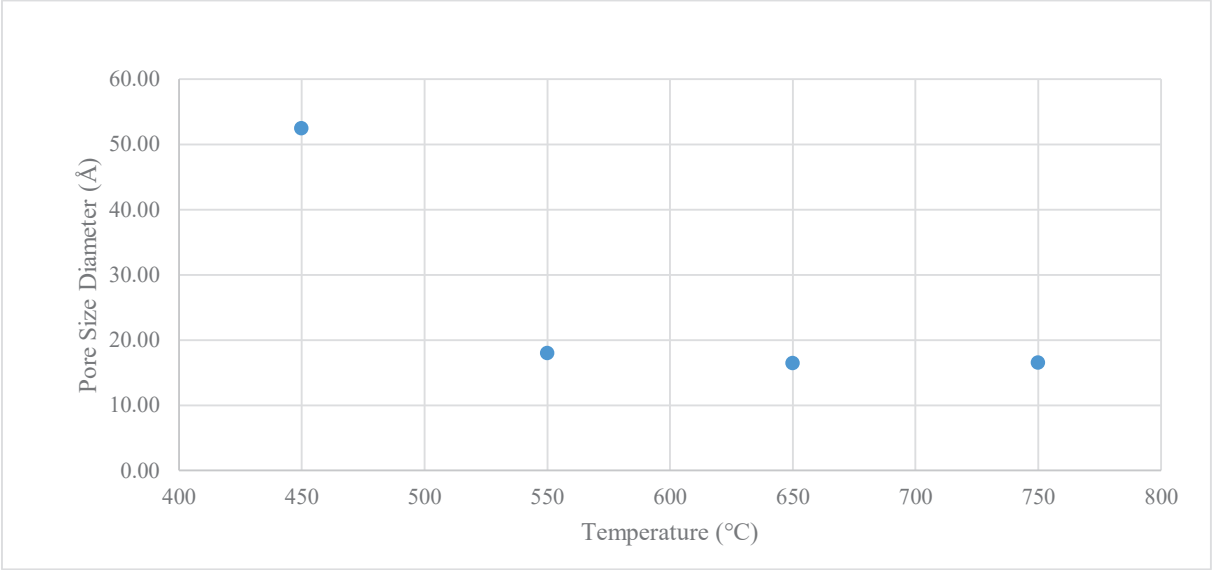

Figure 14: Biochar pore size diameter graphed as a function of temperature

Effect of Temperature on Chemical Functionality at Constant Time

Figure 15 depicts the combined spectrums obtained using FTIR-ATR for each biochar material listed in Table 6, with the wavelengths of identified functional groups labelled within that figure and defined in Table 7. The raw spectra of each of these materials can be found in Appendix A: Raw FTIR Spectra of Biochar Materials

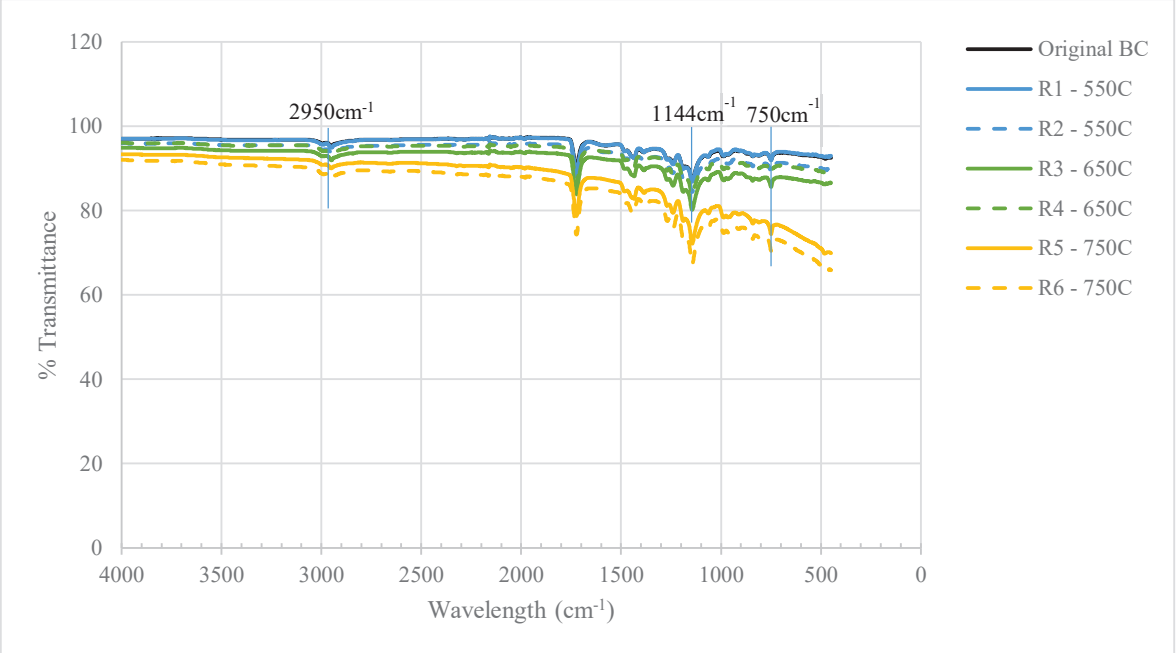

Figure 15: Combined spectrum results from FTIR-ATR

Table 7: Identified absorption wavelengths and corresponding groups from Figure 15

Absorption (cm^{-1})	Group
2950	C-H stretching
1144	C-O stretching
750	C-H bending

3.4 Hydrothermal Modification of Biochar

3.4.1 Methodology

Figure 16: Photograph of Hydrothermal Amar Reactor 1

The hydrothermal reactor, Figure 16, was used to modify the biochar. The hydrothermal reactor operates by subjecting material in a vessel to water and gases under subcritical temperature and pressure conditions, as schematically illustrated in Figure 17.

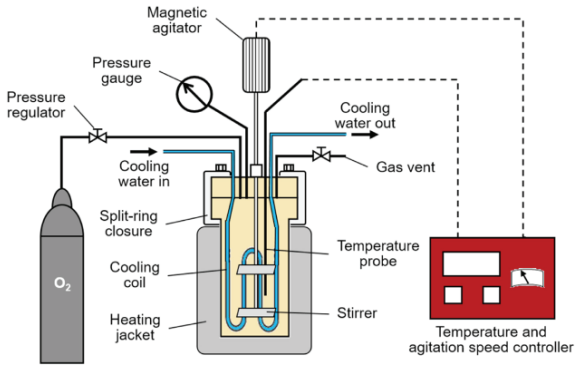

Figure 17: Schematic of Hydrothermal Amar reactor 1

Previously, an oxidative hydrothermal surface modification method for activated carbon was described, and optimal conditions for this treatment were obtained [19]. Surface modification of biochar was used following that treatment method, whose summary follows: 10 g biochar and 100 mL distilled water were loaded into the autoclave reactor and hydrothermally treated at 250°C for 30 minutes under 25 bar pressure of oxygen gas at a stirring speed of 75 rpm. After being retrieved from the reactor, the biochar was rinsed with distilled water and dried at 105°C overnight.

3.4.2 Results

Table 8: Physical Characteristics of Original Biochar, Heat Treated Biochar and Heat Treated Biochar with Hydrothermal Surface Modification

Heat Treatment Condition	SA_{BET} (m^2/g)	V_{micro} (cm^3/g)	Pore Size Diameter (Å)
Original Biochar	1.4388	0.000962	52.4793
Heat Treated Biochar	246.8920	0.136709	13.198
Heat and Hydrothermally Treated Biochar	139.5802	0.081251	<10

Table 8 reports the physical characteristics of the original, heat-treated and hydrothermal biochar.

3.5 Sevoflurane Dynamic Gas Adsorption Measurement

3.5.1 Methodology

Sevoflurane adsorption was measured in a continuous flow system [20]. A schematic of the system is shown in Figure 18, and photographs of the system's components are shown in Figure 19. The system consisted of an Aestiva 5 anaesthetic machine (GE Healthcare, Chicago, Illinois, US) equipped with a Tec™ 7 Vaporiser (GE Healthcare, Chicago, Illinois, US), an E-CAiOV infrared gas module (GE Healthcare, Chicago, Illinois, US), a data logger connected to a Microsoft Windows PC and a fixed bed glass column with an internal coating of Teflon (28 mm-O.D. x 24 mm-I.D.). A digital manometer (CA 852, Chauvin Arnoux, Paris, France) was used

to measure the change in pressure across the column. The vaporiser was the controller for sevoflurane concentration, and the anaesthetic machine was the controller for the carrier gas flow rates. The delivery pressure of the gas cylinders was set to 400 kPa. From the outlet of the adsorption column, gas was channelled to the gas module. The data recorder logged this value every 4 seconds, as frequently as its settings allowed.

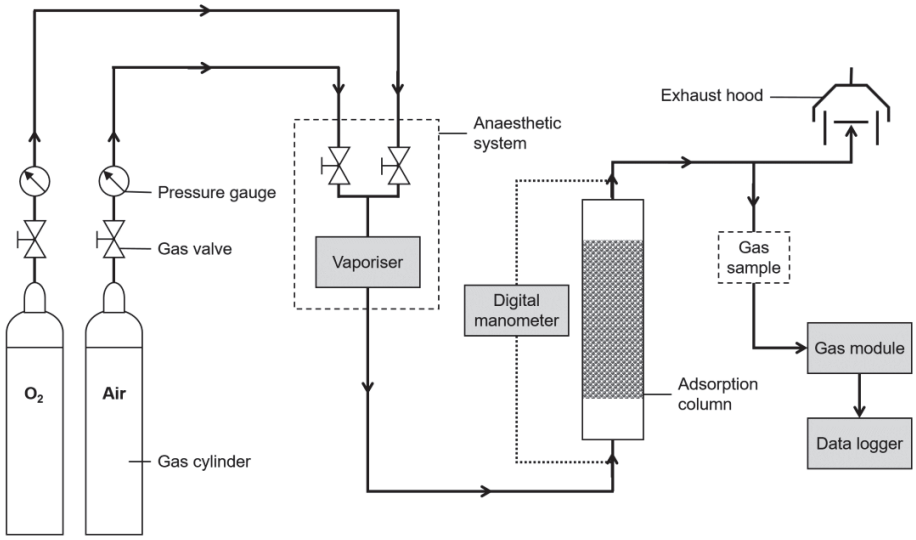

Figure 18: The continuous flow system used for adsorption, [20]

Figure 19: The GE Aestiva 5, the GE TEC™ 7 Vaporiser and the Adsorption Column making up the adsorption system

The labels, conditions and material type for the adsorption experiment runs are tabulated in Table 9. Each condition for the adsorption experiment was duplicated.

Table 9: Adsorption Experimental Runs

Conditions	Flow Rate (L/min)	Bed height (cm)	C_0 (%v/v)	Material Type
1	3	5	1.0	Original Biochar
2	3	5	1.0	Heat-treated Biochar
3	3	5	1.0	Hydrothermally treated biochar

The adsorption capacity (mg/g adsorbent) was calculated by determining the difference in mass between the adsorption column before and after saturation of the adsorbent in the fixed bed using a microbalance (Kern & Sohn GmbH, Albstadt, Germany), that is by a gravimetric method. The breakthrough curve of the adsorption system was obtained by plotting the normalised concentration (C_t/C_0) against time. The adsorption experiment lasted until the normalised concentration was close to 1; this duration is the adsorbent saturation time.

The breakthrough curve was fitted using Microsoft Excel's solver functionality to the logistic equation [2.1]. The 5% breakthrough, 95% breakthrough, and saturation times were obtained from this fitted equation.

3.5.2 Results

Figure 20 displays the raw breakthrough curve obtained directly from the experimental apparatus of each of the following materials and their duplicates: Original Biochar, Heat Treated Biochar, and Hydrothermally Treated Biochar, while Figure 21 plots the curves fitted to the logistic equation [2.1].

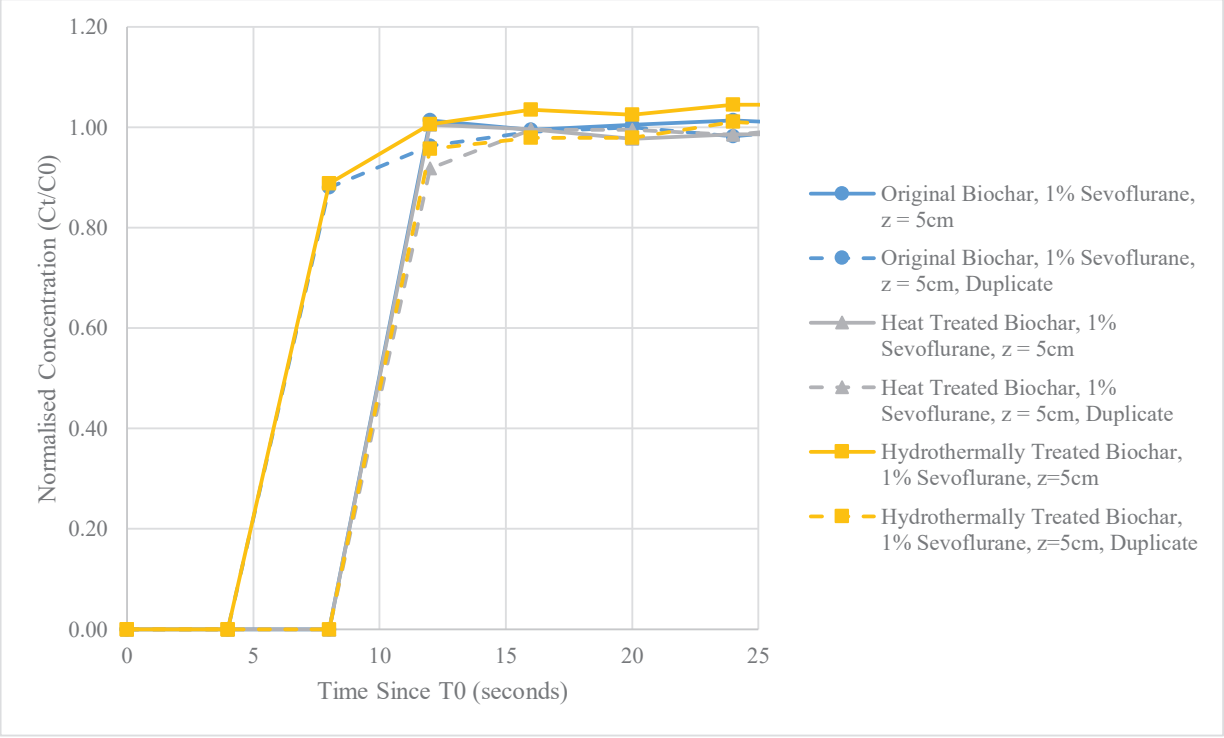

Figure 20: Normalised Concentration vs Time since T0 for Sevoflurane Adsorption on Biochar

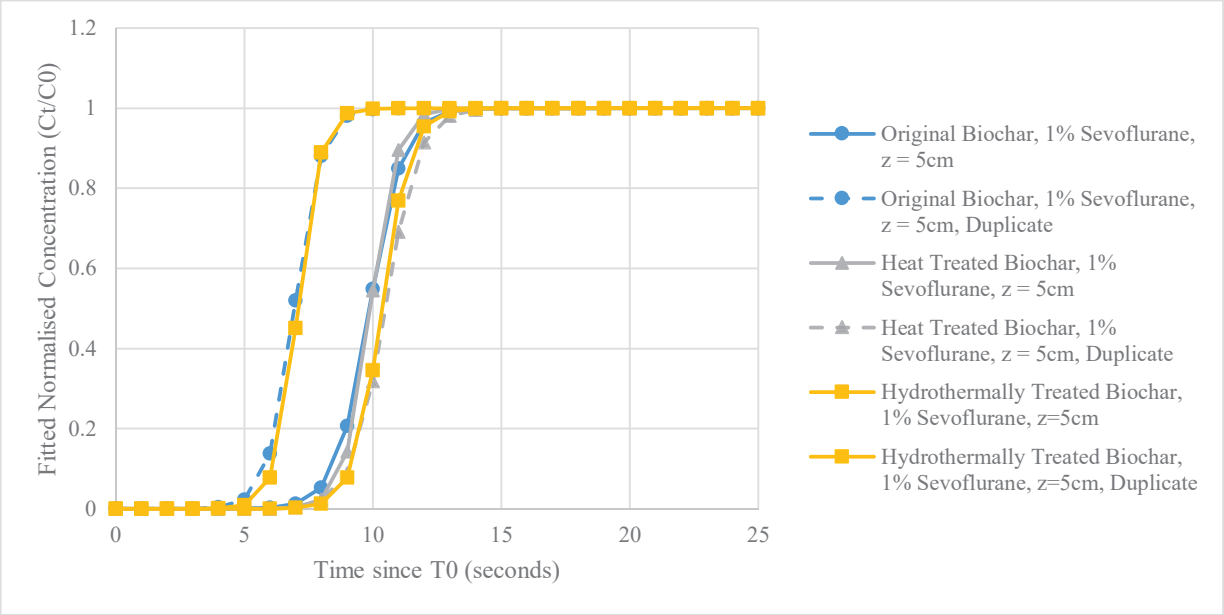

Figure 21: Fitted Logistic Curves for Normalised Concentration vs Time since T0 for Sevoflurane Adsorption on Biochar

From the fitted logistic curve displayed in Figure 21, the breakthrough and saturation times were determined, and these are reported in Table 10, along with the measurement of the gravimetric adsorption capacity.

Table 10: Comparison of Adsorption Capacities, Breakthrough Times, and Saturation Times for Adsorbents

	Adsorption Capacity (mg/g)	5% Breakthrough Time, Average +/- Standard Error (Seconds)	95% Breakthrough Time, Average +/- Standard Error (Seconds)	Saturation Time (Ct/C0 = 0.999999), Average +/- Standard Error (Seconds)
Original Biochar,	0.00	6.69 +/- 1.27	10.14 +/- 1.65	16.52 +/- 2.34
Heat Treated Biochar	0.00	8.51 +/- 0.10	11.88 +/- 0.48	18.11 +/- 1.19
Hydrothermally Treated Biochar	0.00	7.27 +/- 1.48	10.16 +/- 1.78	15.49 +/- 2.34

4 DISCUSSION

4.1 Heat Treatment of Biochar – Optimisation of Conditions

The objective of increasing biochar's surface area and pore size volume was achieved while also retaining the chemical surface functionality of the original biochar. Firstly Table 5 demonstrates that there is very little difference in the physical properties achieved by increasing the heat treatment time to 2 hours from 1 hour, and so from this result, 1 hour was the condition chosen to continue with determining an appropriate heat treatment temperature.

Secondly, concerning Figure 12, there is a quadratic relationship between apparent specific surface area and increasing temperature, with the maximum of 509 m^2/g being achieved at 699.76°C. There is also a quadratic relationship between the micropore volume and increasing temperature, with the maximum of 0.1713 cm^3/g occurring at 727.9°C, as shown in Figure 13. Unlike these two previous physical properties, the pore size diameter approaches a plateauing value of approximately 16.47 Å as temperature increases, Figure 14. These three figures were produced from the data contained in Table 6.

The FTIR-ATR spectra, Figure 15, shows the combined spectra of each of the heat-treated biochars at the three temperatures and the original biochar for comparison. From this figure, it was concluded that biochars up to 650°C have similar chemical functionality, both to each other and to the original biochar, which has not been subject to further heat treatment. At a temperature of 750°C, there is a change in the surface chemistry such that lower wavelength peaks of approximately 750 cm^{-1} become more pronounced when compared to the original biochar. These low-wavelength peaks were interpreted to be characteristic of C-H groups. Because it was known from the COSMO-RS modelling within [19] that C-H groups were not conducive to anaesthetic agent adsorption, it was concluded that biochars with these characteristic spectra were unsuitable for adsorbing anaesthetics. Additionally, from [40], it was learned that after 700°C, the biochar structure undergoes a transition to have an increasing proportion of turbostratic crystallite making up its structure.

This process stage concluded with choosing a temperature below 700° to obtain sufficient biochar for adsorption experiments. For the best conditions, a temperature of 650°C was decided upon because heat-treated biochar had been proven to have appropriate physical properties and surface chemistry at this temperature.

4.2 Heat Treatment of Biochar using Best Conditions

With the best conditions for an adsorption trial decided upon, sufficient biochar for that trial needed to be heat treated. The results, reported in Table 8, showed a significant increase in the specific surface area and micropore volume, with the values increasing from 1.439 to 246.9 m^2/g and from 0.00096 to 0.137cm^3/g between the original biochar and the heat-treated biochar, respectively. However, this increase was not as significant as the results obtained during the process's optimisation of conditions. This difference is likely because the same size

crucible was used for both heat treatments, making the issue related to scale-up and similitude. In particular, the filled crucible had a lower ratio of available surface area for mass transfer relative to the volume of particles contained in it than the half-full crucible.

4.3 Hydrothermal Modification of Biochar

Table 8 also reports the physical properties of heat-treated biochar hydrothermally treated in an oxidative environment, which shows that the apparent specific surface area, micropore volume and pore size diameter have decreased. This decrease could be because the additional hydrothermal treatment has caused the pores to collapse or become clogged with material, biochar or water.

4.4 Sevoflurane Dynamic Gas Adsorption Measurement

As reported in Table 8, none of the biochar materials tested provides any adsorption capacity for sevoflurane when that adsorption capacity is measured gravimetrically. Although there are differences in the estimated breakthrough and saturation times, because the adsorbent material does not uptake any material, this must solely be due to the adsorbent bed providing a barrier to fluid flow through the column. Compared to the results for activated carbon reported in [20], it is clear that the time for breakthrough and saturation is too short for biochar to be a suitable adsorbent for this application. For example, those results display a graph with a saturation time over 5 minutes for activated carbon at a flow rate of 3L/min and a bed height of 5cm, rather than the 15 seconds reported in Table 10 for hydrothermally treated biochar under the same conditions.

The original biochar had poor performance, but this was expected because it has a low apparent specific surface area and a minute pore volume, hence the executed improvement activities to improve these properties. The poor performance of the heat-treated biochar was surprising because of its physical properties. The final heat-treated material had a specific surface area of 246.9 m^2/g and a pore volume of 0.137cm^3/g, indicating that the improvement activities were successful in improving the properties but not successful in improving the function. One explanation is that the pore diameter is too small to allow gas diffusion into the pores. From Table 1, sevoflurane has a kinetic diameter of 7.1 Å, whereas, in Table 8, the pore size diameter of the heat-treated biochar is 13.2 Å. It could be that there is a geometric incompatibility between the size of the pores and the target molecule.

Another explanation is that the surface chemistry of the biochar is inappropriate to adsorb sevoflurane due to the non-polar nature of that molecule.

5 CONCLUSIONS

5.1 Conclusions

Contrary to initially held expectations, and despite having attractive economic and environmental qualities, the biochar material does not perform well in the intended application of sevoflurane adsorption. Further altering the surface area of the biochar through heat treatment made no discernable difference to the gravimetric adsorption capacity of the material within a dynamic adsorption system, and neither did a hydrothermal modification of the biochar. This lack of performance is likely because of geometric incompatibilities between the target molecule and pore size, with an additional factor being the target molecule's relative lack of chemical interactions with other substances, including biochar.

Therefore, the material with the best performance in the current application is the activated carbon previously determined, and recommendations will be made based on this conclusion.

5.2 Recommendations for future research

5.2.1 Valorising waste material – use as a soil amendment or convert biochar to activated carbon.

When produced as a waste product of another process, like fast pyrolysis, biochar is a stream of material that could be valorised and further utilised. Either biochar could be used as a soil amendment and fertiliser or converted to another material. For example, biochar could be further processed into valuable carbon-based materials, such as activated carbon. A potential avenue of further research is to explore the engineering of biochar as a value-added product and whether further transformations are technically, economically, societally and environmentally feasible and desirable, focusing on how these aspects of the transformation compared to the next best alternative of returning the biochar to the soil where the biomass was grown.

5.2.2 Different methods for surface functionalisation

The COSMO-RS models from previous work predict that specific surface functionalities have distinct adsorption abilities. Therefore, more materials surface engineering work could be done to remove the detrimental surface functionalities while keeping or adding additional beneficial surface functionalities. At the same time, this modification cannot come at the expense of physical properties such as surface area, pore volume and pore size, so more work needs to be done to carefully control these surface functionalities while retaining or enhancing the physical properties that make the adsorbent desirable. That research question could be addressed for engineered biochar and activated carbon material.

5.2.3 Economic analysis

It has already been demonstrated that activated carbon is a technically effective adsorbent of volatile anaesthetic agents. The question remains whether activated carbon is economically viable as an adsorbent of volatile anaesthetic agents, be it unmodified activated carbon or modified activated carbon. Further engineering the activated carbon to adsorb the anaesthetic agent more effectively could negatively affect the economic viability of such a solution purely because the cost of improving the adsorbent properties does not yield an appropriate increase in adsorption ability. In other words, the activated carbon could become wastefully processed relative to its intended application.

As an economic factor, there is also the question of establishing a viable and sustainable model for downstream processes for purifying and either using or disposing of the anaesthetic agents. Additionally, a commercial service delivery model, particularly for the recovery of the waste anaesthetic agent, needs to be developed before the technology can be applied.

5.2.4 Advocacy and advertising of a separation solution to the medical community

The goal of capturing anaesthetic agents from anaesthetic procedures will never be achieved unless the technology is disseminated into medical practice locally, in New Zealand, or globally. There is awareness within the medical community of the anaesthetic agent emissions problem, and conversations are occurring that concern solutions practically introducible by individual anaesthetists operating within the hospital system. However, for the most part, these discussions make no mention of the work being conducted by scientists and engineers to achieve the goal of capturing anaesthetic agents. Therefore, more work needs to be done to communicate across professional domains so that potential users of the capturing technology know it exists. Moreover, more work needs to be done to make it convenient to access this technology.

5.2.5 Assess materials under applicable conditions.

The suggested application is to capture anaesthetic agents from the exhaled breath of patients undergoing procedures involving anaesthesia. Therefore, for relevant comparison to the final application, materials must be tested under the conditions in which they are to be used. For example, exhaled breath contains high levels of water vapour, and the adsorbent must not suffer from detrimental effects when exposed to humidity. Furthermore, the influent containing the anaesthetic agent to be adsorbed is likely to be moving, so a dynamic adsorption system is preferred for experiments and demonstrations of efficacy. While static adsorption experiments are helpful to screen materials, these do not resemble the final application of the adsorbents. Thus, humid and dynamic flow conditions are required to prove the efficacy of materials. One possible improvement to the apparatus used in this experiment is to introduce humidity.

5.2.6 Scaling up adsorbent system

The dynamic adsorption system needs to be scaled up for activated carbon to demonstrate the system working at a larger scale. A larger system would have more capacity for adsorbate and, therefore, an increased time before the adsorbent breakthrough is achieved and the system needs to be regenerated. However, the scale-up would affect other operating parameters, such as the pressure drop across the adsorbent bed. Therefore, a larger apparatus needs to be tested to ensure that the system still gives adequate performance for the intended application. If this step is successful, the adsorbent system needs to be tested in its intended role in a real hospital environment with appropriate personnel and staff responsible for it.

5.2.7 Desorption and Recovery of Anaesthetic from Adsorbent

After a system has successfully captured the anaesthetic agent, downstream processes must be introduced to regenerate the adsorbent material and separate and purify the anaesthetic agent safely and responsibly. Additionally, the destination of the sevoflurane needs to be determined. For example, sevoflurane could be repackaged as a generic medication, but is this safe, ethical and culturally appropriate from the perspective of the future patient? Alternatively, it could be sterilised, chemically deconstructed, and used to manufacture new chemicals from the circular economy perspective, but is this economically and technically feasible? The potential area of demonstrating the techno-economic feasibility of the downstream processes is ripe for exploration.

5.2.8 Is adsorptive capture the most appropriate mechanism?

Finally, the target molecule, sevoflurane, only has weak interactions with other molecules, as it is non-polar and relatively inert. These properties contribute to the safety and efficacy of sevoflurane when used as an anaesthetic agent. However, when approaching the problem from the first principles, these properties could mean that sevoflurane is perhaps unsuited to being captured by a physiochemical surface phenomenon like adsorption, which relies on these interactions to be effective. Other alternative mechanisms are available that could result in a more effective system for this application, and these could be explored further. If the objective is to capture sevoflurane and prevent it from being emitted to the atmosphere, then the entire solution space should be explored.

As has already been mentioned, one example of proven technology in this solution space is membrane technology. Therefore, potential avenues for further research could be to fabricate and test a membrane system that allows large molecules, such as sevoflurane and compound A, to exit the anaesthetic circuit while preventing them from entering the atmosphere.

6 REFERENCES

[1] A. C. Brown *et al.*, "Tropospheric lifetimes of halogenated anaesthetics," *Nature.,* vol. 341, no. 6243, pp. 635-637, 1989, doi: 10.1038/341635a0
info:doi/10.1038/341635a0.

[2] E. Bertram-Ralph and M. Amare, "Inhalational anaesthesia," *Anaesthesia and intensive care medicine,* vol. 23, no. 1, pp. 60-68, 2022, doi: 10.1016/j.mpaic.2021.10.003.

[3] Edmond, "New Inhaled Anesthetics," *Anesthesiology,* vol. 80, no. 4, pp. 906-922, 1994, doi: 10.1097/00000542-199404000-00024.

[4] R. Lopes, C. Shelton, and M. Charlesworth, "Inhalational anaesthetics, ozone depletion, and greenhouse warming: the basics and status of our efforts in environmental mitigation," *Current opinion in anaesthesiology,* vol. 34, no. 4, pp. 415-420, 2021, doi: 10.1097/ACO.0000000000001009.

[5] M. K. Vollmer *et al.*, "Modern inhalation anesthetics: Potent greenhouse gases in the global atmosphere," *Geophysical Research Letters,* vol. 42, no. 5, pp. 1606-1611, 2015, doi: 10.1002/2014gl062785.

[6] C. R. Guetter *et al.*, "Greening the operating room," *The American journal of surgery,* vol. 216, no. 4, pp. 683-688, 2018, doi: 10.1016/j.amjsurg.2018.07.021.

[7] T. N. Ang, S. Baroutian, B. R. Young, M. M. Hyland, M. Taylor, and R. Burrell, "Adsorptive separation of volatile anaesthetics: A review of current developments," *Separation and purification technology,* vol. 211, pp. 491-503, 2019, doi: 10.1016/j.seppur.2018.10.012.

[8] L. Liu, F. McGain, and S. E. Kentish, "Recovery of Sevoflurane Anesthetic Gas Using an Organosilica Membrane in Conjunction with a Scavenging System," *Environmental science & technology,* vol. 55, no. 5, pp. 3362-3367, 2021, doi: 10.1021/acs.est.1c00159.

[9] L. Delgado-Herrera, R. D. Ostroff, and S. A. Rogers, "Sevoflurane: approaching the ideal inhalational anesthetic a pharmacologic, pharmacoeconomic, and clinical review," *CNS drug reviews,* vol. 7, no. 1, pp. 48-120, 2001.

[10] "Sevoflurane." https://pubchem.ncbi.nlm.nih.gov/compound/Sevoflurane (accessed 1/05/2022.

[11] E. Frink and B. Brown, "Sevoflurane," *Baillière's clinical anaesthesiology,* vol. 7, no. 4, pp. 899-913, 1993.

[12] C. J. Young and J. L. Apfelbaum, "Inhalational anesthetics: desflurane and sevoflurane," *Journal of clinical anesthesia,* vol. 7, no. 7, pp. 564-577, 1995.

[13] M. Behne, H.-J. Wilke, and S. Harder, "Clinical pharmacokinetics of sevoflurane," *Clinical pharmacokinetics,* vol. 36, no. 1, pp. 13-26, 1999.

[14] I. Smith, M. Nathanson, and P. F. White, "Sevoflurane-a long-awaited volatile anaesthetic," *British Journal of Anaesthesia,* vol. 76, no. 3, pp. 435-445, 1996/03/01/ 1996, doi: https://doi.org/10.1093/bja/76.3.435.

[15] D. O'Hagan, "Understanding organofluorine chemistry. An introduction to the C–F bond," *Chemical Society Reviews,* 10.1039/B711844A vol. 37, no. 2, pp. 308-319, 2008, doi: 10.1039/B711844A.

[16] T. N. Ang *et al.*, "Enrichment of surface oxygen functionalities on activated carbon for adsorptive removal of sevoflurane," *Chemosphere,* vol. 260, p. 127496, Dec 2020, doi: 10.1016/j.chemosphere.2020.127496.

[17] T. N. Ang, "Adsorptive Removal of Volatile Anaesthetics from Waste Medical Gas," 2021. [Online]. Available: https://hdl.handle.net/2292/54586

[18] T. N. Ang *et al.*, "A techno-economic-societal assessment of recovery of waste volatile anaesthetics," *Separation and purification technology,* vol. 226, pp. 304-314, 2019, doi: 10.1016/j.seppur.2019.06.011.

[19] T. N. Ang, B. R. Young, R. Burrell, M. Taylor, M. K. Aroua, and S. Baroutian, "Oxidative hydrothermal surface modification of activated carbon for sevoflurane removal," *Chemosphere,* vol. 264, no. Pt 2, p. 128535, Feb 2021, doi: 10.1016/j.chemosphere.2020.128535.

[20] T. N. Ang, B. R. Young, M. Taylor, R. Burrell, M. K. Aroua, and S. Baroutian, "Breakthrough analysis of continuous fixed-bed adsorption of sevoflurane using activated carbons," *Chemosphere (Oxford),* vol. 239, p. 124839, 2020, doi: 10.1016/j.chemosphere.2019.124839.

[21] T. Nam Ang, B. R. Young, M. Taylor, R. Burrell, M. Kheireddine Aroua, and S. Baroutian, "Tailoring of activated carbon with ammonia for enhanced anaesthetic sevoflurane adsorption," *Separation and Purification Technology,* vol. 251, 2020, doi: 10.1016/j.seppur.2020.117404.

[22] M. Mehrata, C. Moralejo, and W. A. Anderson, "Adsorbent comparisons for anesthetic gas capture in hospital air emissions," *Journal of environmental science and health. Part A, Toxic/hazardous substances & environmental engineering,* vol. 51, no. 10, pp. 805-809, 2016, doi: 10.1080/10934529.2016.1181438.

[23] D. Bucher, C. Pasel, M. Luckas, and D. Bathen, "Adsorption of the Inhalation Anesthetic Isoflurane from Dry and Humid Atmosphere," *Chemical engineering & technology,* vol. 42, no. 6, pp. 1268-1275, 2019, doi: 10.1002/ceat.201900072.

[24] J. Doyle, R. Byrick, D. Filipovic, and F. Cashin, "Silica zeolite scavenging of exhaled isoflurane: A preliminary report," *Canadian journal of anesthesia,* vol. 49, no. 8, pp. 799-804, 2002, doi: 10.1007/BF03017411.

[25] J. Jänchen, J. B. Brückner, and H. Stach, "Adsorption of desflurane from the scavenging system during high-flow and minimal-flow anaesthesia by zeolites," *European journal of anaesthesiology,* vol. 15, no. 3, pp. 324-329, 1998, doi: 10.1046/j.1365-2346.1998.00299.x.

[26] D. Bucher, C. Pasel, M. Luckas, J. r. Bentgens, and D. Bathen, "Adsorption of Inhalation Anesthetics (Fluranes and Ethers) on Activated Carbons and Zeolites at Trace Level Concentrations," *Journal of chemical and engineering data,* vol. 62, no. 6, pp. 1832-1841, 2017, doi: 10.1021/acs.jced.7b00079.

[27] N. Gargiulo *et al.*, "A chromium-based metal organic framework as a potential high performance adsorbent for anaesthetic vapours," *RSC advances,* vol. 4, no. 90, pp. 49478-49484, 2014, doi: 10.1039/c4ra05905k.

[28] S. Y. Song, B. R. Lim, and T. Ryu, "Adsorption of desflurane by the silica gel filters in breathing circuits: an in vitro study," *Korean J Anesthesiol,* vol. 68, no. 3, pp. 274-280, 6 2015, doi: 10.4097/kjae.2015.68.3.274.

[29] T.-H. Chen, W. Kaveevivitchai, A. J. Jacobson, and O. E. Miljanić, "Adsorption of fluorinated anesthetics within the pores of a molecular crystal," *Chemical communications (Cambridge, England),* vol. 51, no. 74, pp. 14096-14098, 2015, doi: 10.1039/c5cc04885k.

[30] Y. Hua, N. Gargiulo, A. Peluso, P. Aprea, M. Eić, and D. Caputo, "Adsorption Behavior of Halogenated Anesthetic and Water Vapor on Cr-Based MOF (MIL-101) Adsorbent. Part I. Equilibrium and Breakthrough Characterizations," *Chemie ingenieur technik,* vol. 88, no. 11, pp. 1730-1738, 2016, doi: 10.1002/cite.201600051.

[31] K. H. Chu, "Comments on "Breakthrough analysis of continuous fixed-bed adsorption of sevoflurane using activated carbons"," *Chemosphere (Oxford),* vol. 247, pp. 125841-125841, 2020, doi: 10.1016/j.chemosphere.2020.125841.

[32] M. D. Levan, G. Carta, J. A. Ritter, and K. S. Walton, "Section 16: Adsorption and Ion Exchange," *Perry's Chemical Engineers' Handbook, 9th Edition*, D. W. Green and M. Z. Southard, Eds., 9th edition. ed.: McGraw-Hill Education, 2018, p. 1 online resource (2352 pages). [Online]. Available: https://www.accessengineeringlibrary.com/browse/perrys-chemical-engineers-handbook-9th-edition

[33] W. L. McCabe, J. C. Smith, and P. Harriott, *Unit operations of chemical engineering*, Seventh edition / ed. Boston: McGraw-Hill, 2005, pp. xxv, 1140 pages.

[34] C. A. Simmons and EBSCOhost, *Biochar : chemical composition, soil applications and ecological impacts*. pp. 1 online resource (ix, 107 pages.).

[35] K. Weber and P. Quicker, "Properties of biochar," *Fuel,* vol. 217, pp. 240-261, 2018, doi: 10.1016/j.fuel.2017.12.054.

[36] M. S. Reza *et al.*, "Preparation of activated carbon from biomass and its' applications in water and gas purification, a review," *Arab journal of basic and applied sciences,* vol. 27, no. 1, pp. 208-238, 2020, doi: 10.1080/25765299.2020.1766799.

[37] B. Wang, B. Gao, and J. Fang, "Recent advances in engineered biochar productions and applications," *Critical Reviews in Environmental Science and Technology,* vol. 47, no. 22, pp. 2158-2207, 2017/11/17 2017, doi: 10.1080/10643389.2017.1418580.

[38] M. T. Moreira, I. Noya, and G. Feijoo, "The prospective use of biochar as adsorption matrix - A review from a lifecycle perspective," *Bioresource technology,* vol. 246, pp. 135-141, 2017, doi: 10.1016/j.biortech.2017.08.041.

[39] P. Krasucka, B. Pan, Y. Sik Ok, D. Mohan, B. Sarkar, and P. Oleszczuk, "Engineered biochar - A sustainable solution for the removal of antibiotics from water," *Chemical engineering journal (Lausanne, Switzerland : 1996),* vol. 405, p. 126926, 2021, doi: 10.1016/j.cej.2020.126926.

[40] M. Keiluweit, P. S. Nico, M. G. Johnson, and M. Kleber, "Dynamic Molecular Structure of Plant Biomass-Derived Black Carbon (Biochar)," *Environmental science & technology,* vol. 44, no. 4, pp.

1247-1253, 2010, doi: 10.1021/es9031419.
[41] X. Xin, K. Dell, I. A. Udugama, B. R. Young, and S. Baroutian, "Transforming biomass pyrolysis technologies to produce liquid smoke food flavouring," *Journal of Cleaner Production,* vol. 294, p. 125368, 2021/04/20/ 2021, doi: https://doi.org/10.1016/j.jclepro.2020.125368.
[42] S. Brunauer, P. H. Emmett, and E. Teller, "Adsorption of Gases in Multimolecular Layers," *Journal of the American Chemical Society,* vol. 60, no. 2, pp. 309-319, 1938, doi: 10.1021/ja01269a023.
[43] B. C. Lippens and J. H. de Boer, "Studies on pore systems in catalysts: V. The t method," *Journal of Catalysis,* vol. 4, no. 3, pp. 319-323, 1965/06/01/ 1965, doi: https://doi.org/10.1016/0021-9517(65)90307-6.

Appendix A: Raw FTIR Spectra of Biochar Materials

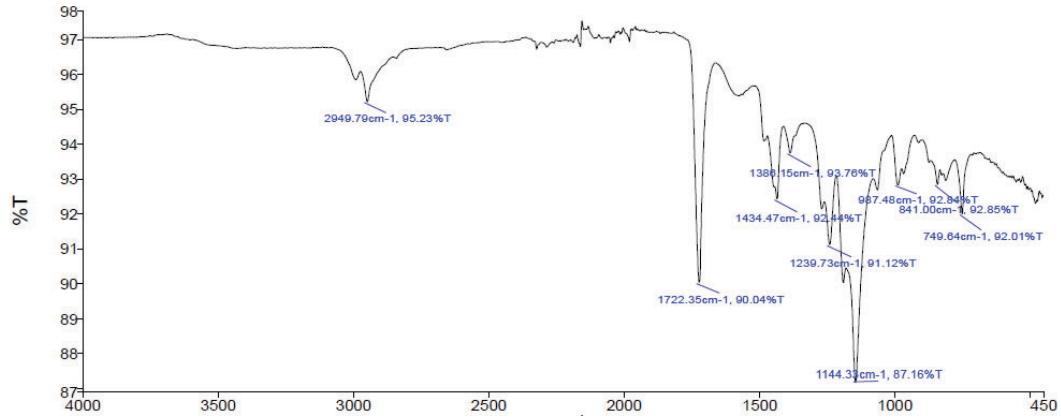

Figure 22: FTIR Spectrum for Original Biochar

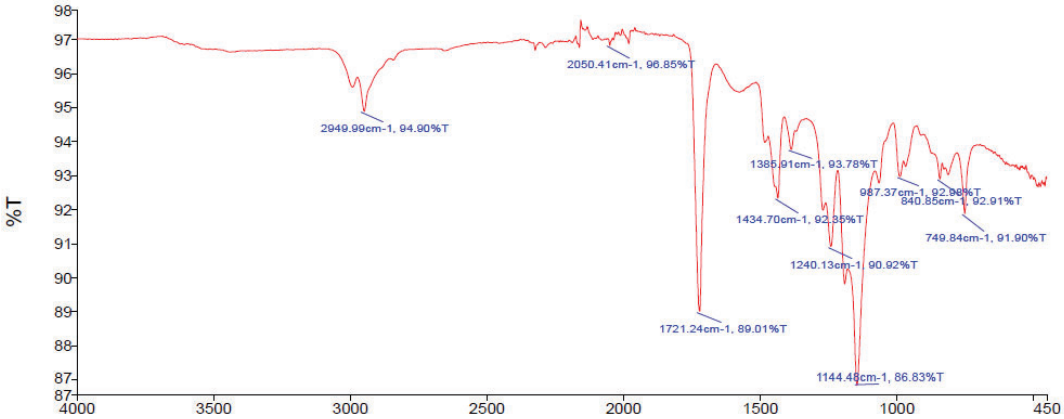

Figure 23: FTIR Spectrum for R1 – 550C

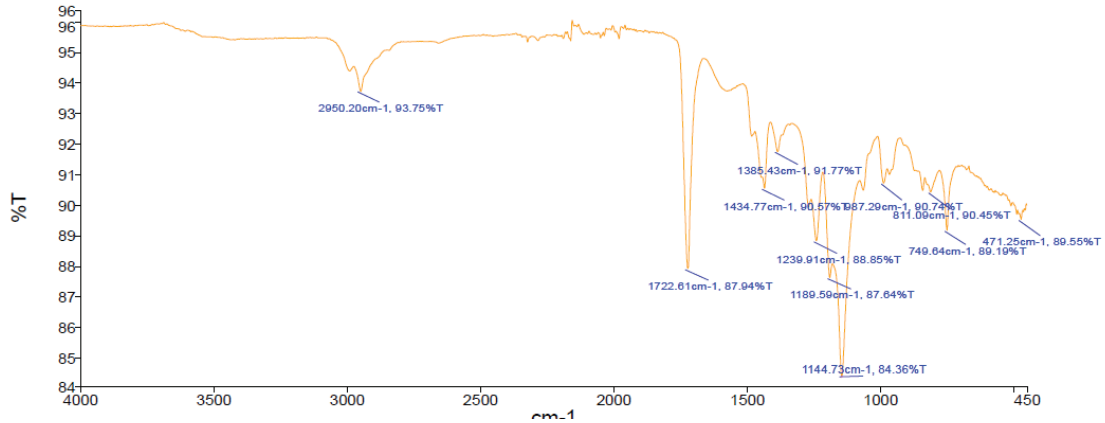

Figure 24: FTIR Spectrum for R2 – 550C

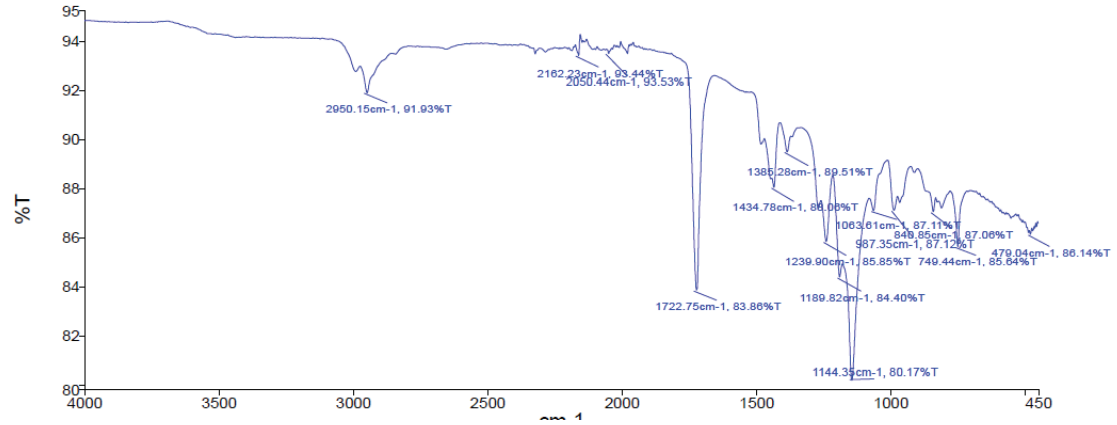

Figure 25: FTIR Spectrum for R3 - 650C

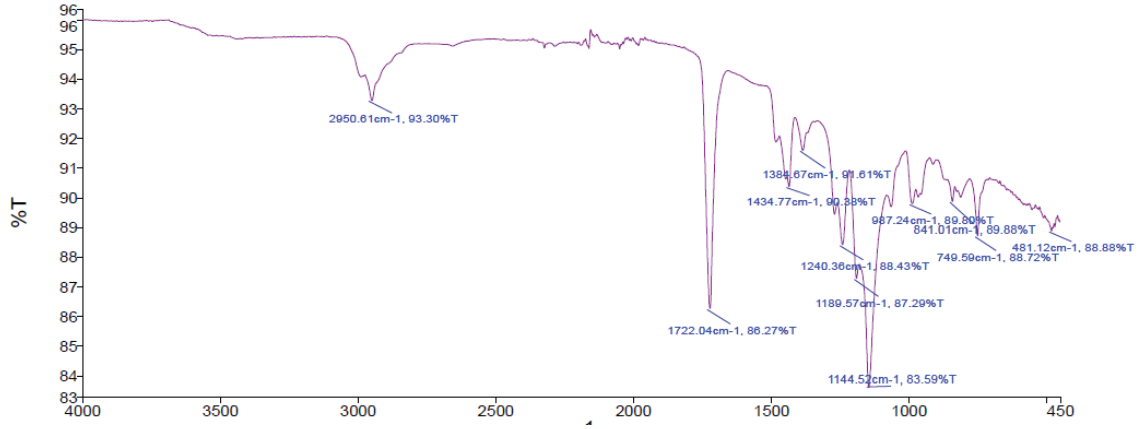

Figure 26: FTIR Spectrum for R4 - 650C

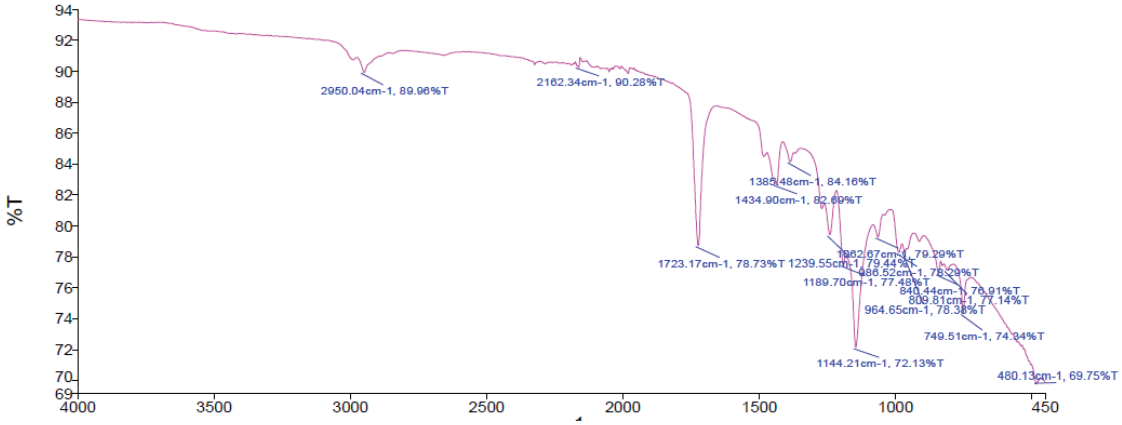

Figure 27: FTIR Spectrum for R5 - 750C

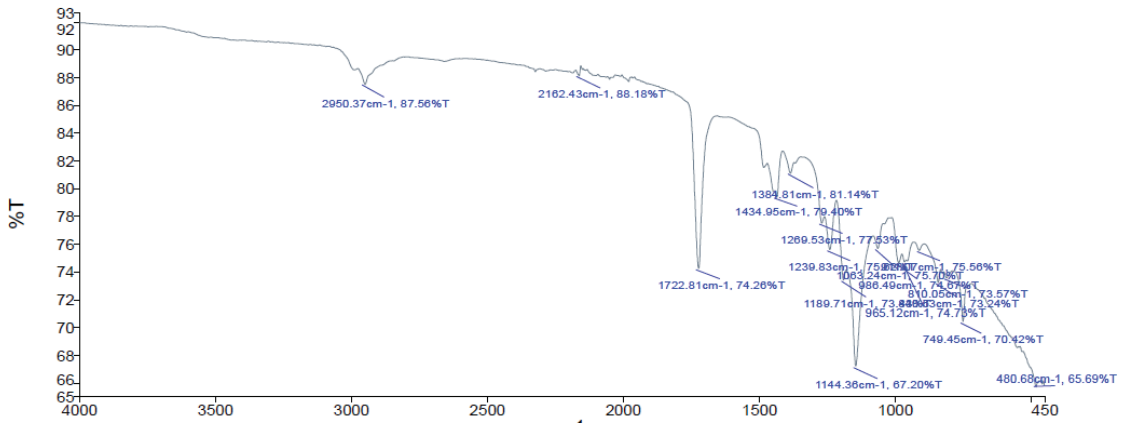

Figure 28: FTIR Spectrum for R6 - 750C